MULTIOBJECTIVE OPTIMIZATION OF THE 3D TOPOLOGICAL ACTIVE VOLUME SEGMENTATION MODEL

Jorge Novo, Manuel G. Penedo and José Santos

Computer Science Department, University of A Coruña, Campus de Elviña s/n 15071, A Coruña, Spain

Keywords: Deformable segmentation models, Genetic algorithms, Evolutionary multiobjective optimization.

Abstract: In this work it is proposed an evolutionary multiobjective methodology for the optimization of topological active volumes. This is a 3D deformable model that integrates features of region-based and boundary-based segmentation techniques. The model deformation is controlled by energy functions that must be minimized. Most optimization algorithms need an experimental tuning of the energy parameters of the model in order to obtain the best adjusted segmentation.
To avoid the step of the parameter tuning, we developed an evolutionary multiobjective optimization that considers the optimization of several objectives in parallel. The proposed methodology is based on the SPEA2 algorithm, adapted to our application, to obtain the Pareto optimal individuals. The proposed method was tested on several representative images from different domains yielding highly accurate results.

1 INTRODUCTION

The active nets model (Tsumiyama and Yamamoto, 1989) was proposed as a variant of the deformable models (Kass et al., 1988) that integrates features of region–based and boundary–based segmentation techniques. To this end, active nets distinguish two kinds of nodes: internal nodes, related to the region–based information, and external nodes, related to the boundary–based information. The former model the inner topology of the objects whereas the latter fit the edges of the objects.

The Topological Active Net model and its extension to 3D, that is, the Topological Active Volume (TAV) model (Barreira and Penedo, 2005), were developed as an extension of the original active net model. It solves some intrinsic problems to the deformable models such as the initialization problem. The model deformation is controlled by energy functions in such a way that the mesh energy has a minimum when the model is over the objects of the scene. The TAV model is an active model focused on segmentation tasks that makes use of a volumetric distribution of the nodes. It integrates information of edges and regions in the adjustment process and allows to obtain topological information inside the objects found. This way, the model, not only detects surfaces as any other active contour model, but also segments the inside of the objects. The model has a dynamic behavior by means of topological changes

in its structure, that enables accurate adjustments and the detection of several objects in the scene.

There is very little work in the optimization of active models with genetic algorithms (GA), mainly in edge or surface extraction (Ballerini, 1999; Séguier and Cladel, 2003a) in 2D tasks. For instance, in (Ballerini, 1999) the author developed the "genetic snakes", this is, snakes that minimize their energy by means of genetic algorithms. In (Ibáñez et al., 2009) the authors proved the superiority of a global search method by means of a GA in the optimization of the Topological Active Nets model in 2D images. The results showed that the GA is less sensitive to noise than the usual greedy optimizations and does not depend on the parameter set or the mesh size.

Regarding 3D images, the authors in (Jones and Metaxas, 1997) used deformable contours to estimate organ boundaries. They integrated region-based and physics-based boundary estimation methods. Starting from a single voxel within the interior of an object, they made an initial estimate of the objects boundaries using fuzzy affinity, which measures the probability of two voxels belonging to the same object, together with clustering. In (Qiu et al., 2004) the authors used two deformable models: a deformable surface model (SMD) and a Deformable Elastic Template (DET). The main drawback of these models, as the authors indicate, is that in both models an initial shape (surface or ellipsoid) is needed as well as it must be manually positioned in the data/image. The same drawback

can be associated with adaptive deformable models, typically with only surface modelling, which use a reparameterization mechanism that enables the evolution of surfaces in complex geometries. In (McInerney and Terzopoulos, 1999) it is used a model of this type with complex anatomic structures from medical images.

The author in (Bro-Nielsen, 1994) used 3D "active cubes" to segment medical images, where the automatic net division was a key issue. Since the greedy energy-minimization algorithm proposed was sensitive to noise, an improved greedy algorithm inspired by a simulated annealing procedure was also incorporated. In (Novo et al., 2007) the authors proposed a GA with new defined operators for the segmentation process using TAV structures. The genetic approach overcame some drawbacks, basically in images with different types of noise, with regard to the work proposed in (Barreira and Penedo, 2005). The main problem of the TAV model, as in other deformable models, is that it is necessary an experimental tuning of the parameters that weights the different energy components that are used for the optimization of the model. These weights are usually very dependent on the kind of image to segment.

Multiobjective Optimization Algorithms (MOAs) give a solution to this problem by considering the optimization of several objectives in parallel. The MOAs usually work with conflicting objectives trying to identify a set of optimal trade-off solutions or nondominated solutions which is called the *Pareto Set*. Multiobjective Optimization Evolutionary Algorithms (MOEAs) (Deb, 2001; Jaimes and Coello, 2009), use the principles of evolutionary computing to the search of the Pareto Set. We used in this work one of the best-established algorithms of this type, SPEA2 algorithm (Zitzler et al., 2002). We tested the advantages that add the use of the MOEA methodology in the optimization of the active volume deformable models. There is practically no work using MOEAs applied to deformable models. In the work (Séguier and Cladel, 2003b), a multiobjective optimization of different energy components was developed to the optimization of snakes in an audio-visual speech recognition task. The authors optimized two snakes to fit the external and interior lips contours, using only a small limited number of contour points for each snake. After the evaluation of the snakes energy components, the chromosomes were ranked and, this way, the Pareto optimal solutions were searched. According to the authors, the multiobjective optimization required less iterations than an usual genetic optimization.

2 TOPOLOGICAL ACTIVE VOLUMES. DEFINITION OF OBJECTIVES

A Topological Active Volume (TAV) is a discrete implementation of an elastic $n-$dimensional mesh with interrelated nodes (Barreira and Penedo, 2005). The model has two kinds of nodes: internal and external, which represents different object features: the external nodes fit the edges whereas the internal nodes model their internal topology.

As in other deformable models, the state of the model is governed by an energy function, composed of an internal and an external energy term. The internal energy controls the shape and the structure of the net whereas the external energy represents the external forces which govern the adjustment process. These energies are composed of several objectives and in all the cases the aim is their minimization.

Internal Energy Objectives. The internal energy depends on first and second order derivatives which control the contraction and bending of the mesh, respectively:

$$E_{int}(v(r,s,t)) = \alpha(|v_r(r,s,t)|^2 + |v_s(r,s,t)|^2 + |v_t(r,s,t)|^2) + \beta(|v_{rr}(r,s,t)|^2 + |v_{ss}(r,s,t)|^2 + |v_{tt}(r,s,t)|^2) + 2\gamma(|v_{rs}(r,s,t)|^2 + |v_{rt}(r,s,t)|^2 + |v_{st}(r,s,t)|^2)$$

(1)

where the subscripts represents partial derivatives and α, β and γ are coefficients controlling the first and second order smoothness of the net.

External Energy Objectives. The external energy represents the features of the scene that guide the adjustment process:

$$E_{ext}(v(r,s,t)) = \omega f[I(v(r,s,t))] + \frac{\rho}{\aleph(r,s,t)} \sum_{n \in \aleph(r,s,t)} \frac{1}{\|v(r,s,t)-v(n)\|} f[I(v(n))]$$

(2)

where ω and ρ are weights, $I(v(r,s,t))$ is the intensity value of the original image in the position $v(r,s,t)$, $\aleph(r,s,t)$ is the neighborhood of the node (r,s,t) and f is a function of the image intensity, which is different for both types of nodes. If the objects to detect are bright and the background is dark, the energy of an internal node will be minimum when it is on a position with a high grey level. Also, the energy of an external node will be minimum when it is on a discontinuity and on a dark point outside the object. So, the function f is defined as:

$$f[I(v(r,s,t))] = \begin{cases} IO_i(v(r,s,t)) + \tau IOD_i(v(r,s,t)) \text{ internal nodes} \\ IO_e(v(r,s,t)) + \tau IOD_e(v(r,s,t)) \\ + \xi(G_{max} - G(v(r,s,t))) \\ + \delta GD(v(r,s,t)) \text{ external nodes} \end{cases}$$

(3)

where τ, ξ and δ are weights, G_{max} and $G(v(r,s,t))$ are the maximum gradient of the image and the gradient of the input image in node position $v(r,s,t)$, IO is a term we called "In-Out" and IOD a term called "distance In-Out", and $GD(v(r,s,t))$ is a gradient distance

term. The *IO* terms minimize the energy of those individuals with the external nodes in background intensity values and the internal nodes in object intensity values meanwhile the terms *IOD* act as a gradient: for the internal nodes (IOD_i) its value minimizes towards brighter values of the image, whereas for the external nodes its value (IOD_e) is minimized towards low values (the background).

The greedy (Barreira and Penedo, 2005) and the genetic algorithm (GA) (Ibáñez et al., 2009) aim is the optimization of a global objective defined as the sum of the individual objectives weighted with the exposed parameters: α, β, γ, ω, ρ, ξ, δ and τ. (Novo et al., 2007) includes the definition of the genetic operators used with a GA: arithmetic crossover, mutation of a node, mutation of a group of neighboring nodes, shift of a mesh and spread of a mesh. In the case of the evolutionary Multiobjective Optimization (MO), most of the segmentations will use the following energy terms as independent objectives: the β energy component as a term that provides smoothness, and a summed of IOD_i (only internal nodes) and *GD*. Thus, we merged both compatible properties as only one objective.

3 ADAPTED SPEA2 ALGORITHM

SPEA2 (Zitzler et al., 2002) is an improved version of the *Strength Pareto Evolutionary Algorithm (SPEA)*. The new version incorporates a fine-grained fitness assignment strategy and a density estimation technique. In this section, we describe these two key aspects and our own adaptations.

The algorithm considers, in each generation t, a regular population P_t of size N and an archive $\overline{P}_t$ (external set). This archive contains the nondominated solutions and possibly some dominated solutions if the number of nondominated solutions is less than its size. The size of the archive ($\overline{N}$) is fixed and initially the archive is empty ($\overline{P}_0 = \emptyset$).

The fitness assignment takes into account dominations between individuals and incorporates density information into its calculation. First, a raw fitness $R(i)$ is calculated based on the number of individuals that dominates an individual i:

$$R(i) = \sum_{j \in P_t + \overline{P}_t, j \succ i} S(j) \tag{4}$$

where $S(j)$ represents the "strength" of individual j, that is, the number of individuals it dominates. This raw fitness of an individual i is calculated using the dominations in both the archive and population set. This way, the individuals of the Pareto Set have a

value $R = 0$, whereas a high value of R means that the individual is dominated by many other individuals.

If several nondominated individuals have the same raw fitness, a density estimation is incorporated to discriminate between them. Thereafter, a density $D(i)$ is then calculated:

$$D(i) = \frac{1}{\sigma_i^k + 2} \tag{5}$$

The term σ_i^k represents the distance from i to its $k - th$ nearest neighbor, being $k = \sqrt{N + \overline{N}}$, taking into account any member of the archive set and population. Finally, adding both terms, the individual fitness is calculated as:

$$F(i) = R(i) + D(i) \tag{6}$$

The $k-$distance defined in SPEA2 uses the entire population to calculate the distances (Eq. 5). Instead, we consider only the nondominated ones, because these are the individuals mainly contained in the archive, which is used for producing the new individuals in the new population. We gain speed because we calculate only a small portion of the distances compared to the original algorithm.

Additionally, instead of the original $k-$distance, we calculate an average $k-$distance as follows. First, after sorting the list of distances for each individual in increasing order, we consider only a window of the list represented by the 8th part of the closest individuals. Finally, the distance σ_i^k is an average over the k-distances that represent the 25%, 50%, 75% and 100% positions on that window. That way, the distance σ_i^k gives a more accurate view of the level of neighborhood of an individual, and with emphasis in the immediate neighborhood.

The next step in the algorithm is the environmental selection which defines how the archive maintains the Pareto Front. In each generation we get a new set of nondominated individuals in P_t and $\overline{P}_t$, and the archive must be updated taking into account the fixed size restriction $\overline{N}$. The archive update operation has to consider all possible situations: If the total size of the nondominated set is equal to ($\overline{N}$) all the new nondominated individuals are copied to the archive. If the archive is large, not only the new nondominated individuals are copied to it, but also the best $\overline{N} - |\overline{P}_{t+1}|$ dominated individuals. If it is small, the worst nondominated individuals in terms of fitness are removed until $|\overline{P}_{t+1}| = \overline{N}$, using a truncation operation.

The termination condition is checked next. If it is satisfied, the output is the set of decision vectors represented by the nondominated individuals in $\overline{P}_{t+1}$. If the stopping condition is not met, then mating selection is performed. We used tournament selection with

replacement on $\overline{P}_{t+1}$ to fill the mating pool. Then, recombination and mutation operators are applied to the mating pool setting P_{t+1} to the resulting population.

Concretely, we applied an arithmetical crossover and mutation operators, as well as other *ad hoc* operators previously developed for the optimization of the active model with a GA as proposed in (Novo et al., 2007). Figure 1 shows an example of the arithmetical crossover between two parents to produce two new individuals (TAVs) with average topologies between the two selected parents. Moreover, we incorporated elitism, defined over each objective. This means that we maintain in the next generation (in the external archive) the best individuals that minimize each one of the objectives. By doing this, we maintain the individuals of the extremes of the Pareto Front in the next generation. We used this option with the objectives that the user can consider as the most important to minimize, as can be the case of the IOD_i/GD that optimizes the external contour segmentation.
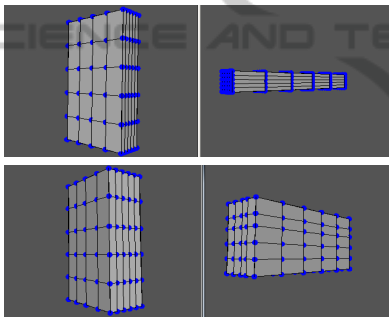

Figure 1: Arithmetical crossover operator. 1st row, selected parents. 2nd row, offspring after the crossover.

4 RESULTS

This section presents some representative results obtained with the methodology developed. To test the method, we selected some representative images taken from different domains: artificial images, that were designed to show its capabilities, and CT images, taken from the medical domain to test the process in a real one. Every image is composed by a given number of slices, normally between 90 and 130, that compose the 3D image. This set is the input to the procedures which calculate the different energy terms.

In the multiobjective processes we used an archive size of 100 individuals and a population size of 2000 individuals. The tournament size was a 3% of the archive size. We also used elitism over the IOD_i/GD objective to keep in the population the individual with the best adjustment to the object contour.

Table 1: TAV parameter sets of the GA 2nd phase in the segmentation processes of the examples.

Figure	α	β	γ	ω	ρ	ξ	δ	τ
3 (b)	2.0	1.5	0.1	1.0	4.5	5.0	10.0	1.0
3 (c)	2.0	1.5	0.1	10.0	4.5	5.0	10.0	10.0

Firstly, we tested the method with artificial images. In Figure 2 the results obtained with different images are shown. The 1st row shows the original image to be segmented or a composing slice (first column), the 3rd row shows an intermediate individual taken from the Pareto Front and 2nd and 4th rows represent the extremes of the Pareto Front for each objective β and IOD_i/GD, respectively. These meshes shown in Figure 2, 2nd row, correspond to the best segmentations regarding the β objective (smoothness) with the optimum values (best possible smoothness) because the procedure creates the initial random TAVs with cubic and regular distributions of the nodes. Nevertheless, although the best individual regarding such objective is present from the beginning, it acts as a point that delimits and forces the progression of the trade-offs nondominated individuals of the Pareto Front. As we can see in the results, the individual that optimizes the IOD_i/GD objective provided the best adjustment to the contour that the process could obtain. In all the trade-offs obtained from the middle of the Pareto Front we can point out the compromise obtained between the smoothness and the contour detection searched in the extremes of the Pareto Front.
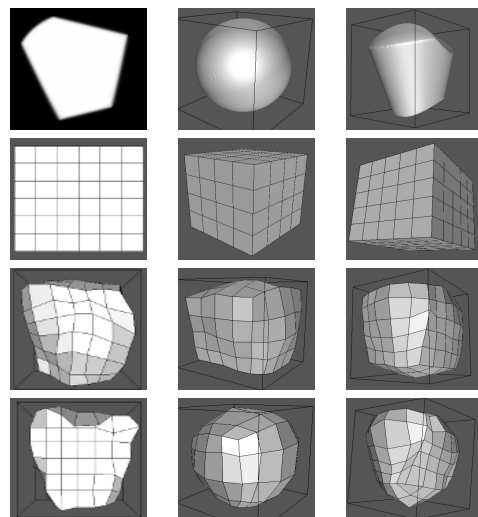

Figure 2: Results obtained in the segmentation of artificial images. 1st row, original image. 2nd row, best individual by β objective. 3rd row, intermediate nondominated individual. 4th row, best individual by IOD_i/GD objective.

We also tested the methodology developed with artificial images specially designed with a higher level

of complexity, in particular containing objects with deep concavities and holes. In Figure 3, two segmentation examples are shown. These 3D images are composed by the given slices repeated over 90 times.

In this case we include the results obtained with a genetic algorithm (GA) to show the main problem of a single-objective optimization procedure. As explained in (Novo et al., 2007) two evolutionary phases are needed: a first evolutionary stage to obtain individuals (TAVs) that detect and cover the object and a second stage to improve the adjustment progressively. The parameters used in the first phase of the GA processes were always the same. The values employed were: $\alpha = 0.00001$, $\beta = 0.00001$, $\gamma = 0.0$, $\omega = 1.0$, $\rho = 1.0$, $\xi = 0.0$, $\delta = 10.0$, $\tau = 0.0$. For the second phase of the GA processes we depict in Table 1 the tuned parameters that were used. The GA used a population size of $2,000$ individuals and a tournament size of 3% of the population. The GA method using a typical parameter configuration (Table 1, first row, parameters tuned for different kinds of no complex images) cannot obtain a correct detection of the holes and concavities. This is shown, for example, in Figure 3, 2nd row, where some internal nodes fall in the hole, which is not correctly delimited. In this case it is necessary to perform a specific tuning of the parameters (Table 1, second row) to detect them (forcing the weight parameters ω and τ to high values), as shown in Figure 3, 3rd row. However, the multiobjective method, due to the IOD_i/GD objective, preserved individuals of the Pareto Front that perform a correct detection in these complex areas. This can be seen in Figure 3, 4th row, representing the best individual from the Pareto Front considering the mentioned objective, IOD_i/GD.

Other kind of images that were used to test the methodology were CT images taken from the medical domain. Thus, we can analyze the segmentation results in a real domain. In Figure 4 three representative examples are shown presenting a high level of complexity or a significant level of noise surrounding the surface of the objects. The proposed method provided a correct segmentation of the objects in these difficult situations. The nondominated individuals correspond to those which minimize the IOD_i/GD objective. Figure 4, 1st row, corresponds to a foot. The input images are noisy CT images of different slices of such foot. Due to the complex surface of this object, we performed a previous stage in this segmentation to obtain a population of individuals that firstly identify the boundary of the foot. This follows the process of 2 stages or evolutionary phases as proposed in (Novo et al., 2007) with a GA. In a first stage, or localization and boundary detection stage, we used IO and GD as
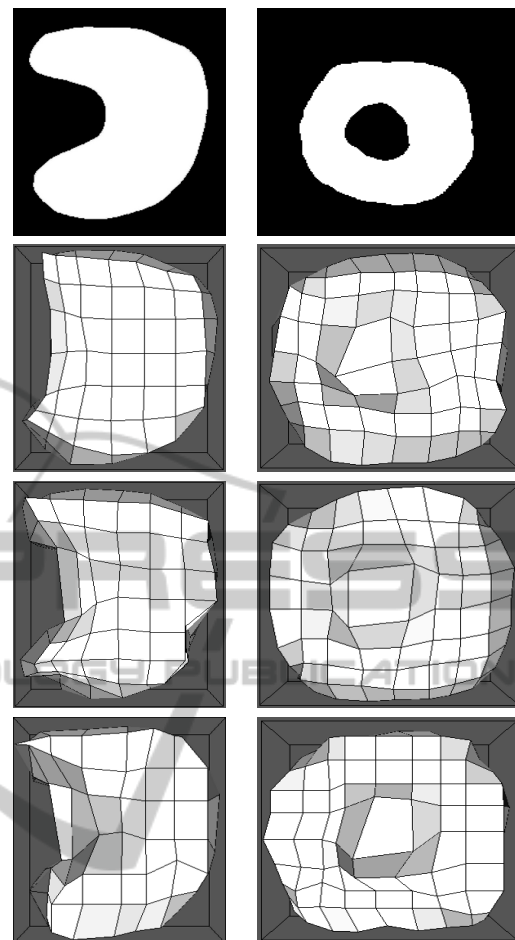

Figure 3: Results obtained in the segmentation of complex objects. 1st row, slice of the original image. 2nd row, final results with the GA method and typical parameters. 3rd row, final results with the GA method and specific parameters. 4th row, nondominated individuals at the end of the evolutionary process.

objectives, and then a second stage to refine the results using the mentioned objectives of β and IOD_i/GD.

The second example corresponds to a vertebra from CT slices. The nondominated selected individual delimits correctly the internal hole, performing a reasonable boundary detection. The third one corresponds to the segmentation of a humerus. In this case, the CT images are very noisy, with an additional external contour (the flesh of the leg) that the optimization method must avoid. Moreover, the boundary of the bone is fuzzy. This can be seen in the final nondominated and selected individual, where a group of external nodes stretch the mesh in a extreme to delimit the brighter area of the bone boundary, as the CT images of such extreme indicate.
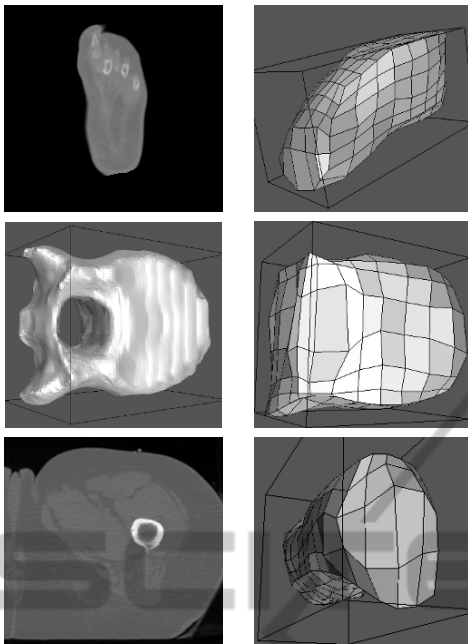
Figure 4: Results obtained in the segmentation with real images. First column, CT slice or 3D reconstruction of the object to segment. Second column, example of nondominated individual at the end of the evolutionary process.

5 CONCLUSIONS

In this paper, we presented a new approach to the energy minimization task in the Topological Active Volume model for image segmentation. The proposed multiobjective method is inspired in the SPEA2 algorithm, being adapted to our specific application. We incorporated the classic genetic operators as well as new ad-hoc ones, including some modifications as a new density estimation technique used to define the fitness of an individual.

The main problem of previous methods for the optimization task, as a greedy algorithm or a GA, is the need of a experimental tuning of the parameters that weight the energy terms in order to obtain correct segmentations in each kind of images. This drawback is directly solved with the multiobjective method. Moreover, our MO approach works with two objectives that summarize all the characteristics we need for a segmentation process (smoothness, boundary adjustment, detection of irregularities), so a single evolutionary phase was required in most of the cases. Additionally, the designer can choose from the final Pareto Front a trade-off segmentation or one which minimizes a particular required objective.

REFERENCES

Ballerini, L. (1999). Medical image segmentation using genetic snakes. In *Proceedings of SPIE: Application and Science of Neural Networks, Fuzzy Systems, and Evolutionary Computation II*, volume 3812, pages 13–23.

Barreira, N. and Penedo, M. G. (2005). Topological Active Volumes. *EURASIP Journal on Applied Signal Processing*, 13(1):1937–1947.

Bro-Nielsen, M. (1994). Active nets and cubes. Technical Report 13, IMM, Technical University of Denmark.

Deb, K. (2001). *Multi-objective optimization using evolutionary algorithms*. Wiley, Chichester, UK.

Ibáñez, O., Barreira, N., Santos, J., and Penedo, M. (2009). Genetic approaches for topological active nets optimization. *Pattern Recognition*, 42:907–917.

Jaimes, A. and Coello, C. (2009). Multi-objective evolutionary algorithms: A review of the state-of-the-art and some of their applications in chemical engineering. In *World Scientific*, pages 61–90.

Jones, T. N. and Metaxas, D. N. (1997). Automated 3D segmentation using deformable models and fuzzy affinity. *15th International Conference on Information Processing in Medical Imaging - LNCS*, 1230:113–126.

Kass, M., Witkin, A., and Terzopoulos, D. (1988). Snakes: Active contour models. *International Journal of Computer Vision*, 1(2):321–323.

McInerney, T. and Terzopoulos, D. (1999). Topology adaptive deformable surfaces for medical image volume segmentation. *IEEE Transactions on Medical Imaging*, 18(10):840–850.

Novo, J., Barreira, N., Santos, J., and Penedo, M. G. (2007). Topological active volumes optimization with genetic approaches. *XII Conference of the Spanish Association for the Artificial Intelligence*, 2:41–50.

Qiu, B., Clarysse, P., Montagnat, J., Janier, M., and Vray, D. (2004). Comparison of 3D deformable models for in vivo measurements of mouse embryo from 3D ultrasound images. In *Ultrasonics Symposium, 2004 IEEE, Vol. 1*, pages 748–751.

Séguier, R. and Cladel, N. (2003a). Genetic snakes: Application on lipreading. In *International Conference on Artificial Neural Networks and Genetic Algorithms*.

Séguier, R. and Cladel, N. (2003b). Multiobjectives genetic snakes: Application on audio-visual speech recognition. In *4th EURASIP Conference*, pages 625–630.

Tsumiyama, K. and Yamamoto, K. (1989). Active net: Active net model for region extraction. *IPSJ SIG notes*, 89(96):1–8.

Zitzler, E., Laumanns, M., and Thiele, L. (2002). SPEA2: Improving the strength pareto evolutionary algorithm. In *EUROGEN 2001, Evolutionary Methods for Design, Optimisation, and Control*, pages 95–100.